Precision Studies of the Higgs Boson Profile at the e^+e^- Linear Collider

Marco Battaglia* and Klaus Desch**

*CERN, CH-1211 Geneva 23 Switzerland
**Universität Hamburg, D-22607 Hamburg Germany

Abstract. This paper reviews the potential of a high luminosity e^+e^- linear collider (LC) in the precision study of the Higgs boson profile. The complementarity of the linear collider data with that from the LHC is also discussed together with a comparison with a muon collider.

I   INTRODUCTION

Explaining the origin of mass is one of the great scientific quests of this turn of the century. The Standard Model (SM), successfully tested to an unprecedented level of accuracy by the LEP and the SLC experiments, addresses this question by the Higgs mechanism [1]. The first manifestation of the Higgs mechanism through the Higgs sector is represented by the existence of at least one Higgs boson. The observation of a new spin-0 particle would represent a first sign that the Higgs mechanism of mass generation is realised in Nature. This motivates a large experimental effort for the Higgs boson search from LEP-2 to the Tevatron and the LHC, actively backed-up by new and more accurate theoretical predictions. After a Higgs discovery, full validation of the Higgs mechanism can only be established by an accurate study of the Higgs boson production and decay properties. This paper discusses the potential of a high luminosity e^+e^- linear collider (LC) in the precision study of the Higgs profile and therefore to the validation of the Higgs mechanism of mass generation. In section II, the status of Higgs searches, through the LEP-2 program, the forthcoming Run-II at the Tevatron and the LHC operation, are shortly discussed and a proof of the observability of the Higgs boson at the linear collider, in the SM and several of its extensions, also accounting for non-standard couplings, is given. Section III outlines the landscape of the Higgs production and decay properties as it is expected to be depicted by the linear collider data. These data will tell about the standard or supersymmetric nature of the observed Higgs and will allow to determine the supersymmetry parameters in the second case. Finally, the complementarity of the linear collider data with what will be learned of the Higgs mechanism in the study of pp collisions at the LHC by 2010 is discussed and the linear collider potential in Higgs physics is compared with that of a muon

collider (FMC).

II THE QUEST FOR THE HIGGS BOSON

The perspectives for the search of the Higgs boson and its detailed study, depend on its mass M_H. In the SM, M_H is expressed as $M_H = \sqrt{2\lambda}v$ where the Higgs field expectation value v is determined in the theory as $(\sqrt{2}G_F)^{-1/2} \approx 246$ GeV, while the Higgs self-coupling λ is not specified, leaving the mass as a free parameter. However, there are strong indications that the mass of the Higgs boson in the SM is light. These are derived from the Higgs self-coupling behaviour at high energies [2], the Higgs field contribution to precision electro-weak data [4] and the results of direct searches at LEP-2 at $\sqrt{s} \geq 206$ GeV and favour the range 113 GeV $< M_H < 206$ GeV.

A From LEP-2 to the LHC

The LEP-2 e^+e^- collider program has been terminated in November 2000 after reaching centre–of–mass energies up to 209 GeV and having collected about 850 pb^{-1} above 200 GeV in its last year of operation. Preliminary results from SM Higgs boson searches [3] have shown an excess of events, consistent with Higgs boson production at a mass of approximately 115 GeV and inconsistent with the expected background at the 2.9σ level when all four LEP experiments are combined. While this observation is certainly not firm enough to be considered as discovery of the Higgs boson, it represents a first direct hint being completely in–line with both the indirect experimental evidence from electro–weak radiative corrections [4] and the theoretical expectations from supersymmetric and grand unified theories.

After the shutdown of LEP, the experimental search for the Higgs boson will continue at the Run II of the Tevatron $p\bar{p}$–collider. The most sensitive search channel for $M_H < 130$ GeV is the $W^{\pm}H$ associated production with $H \to b\bar{b}$ while a significant part of the sensitivity at 130 GeV $< M_H < 180$ GeV comes from the $gg \to H$ process with subsequent $H \to W^{(*)}W$ decays. The combined sensitivity of the two experiments CDF and D0 is shown in figure 1. It is interesting to note that the LEP observation could be ruled out at the 95% confidence level already with an integrated luminosity of about 2 pb^{-1} while a 5σ discovery would require about ten times more luminosity at the same mass. A 3σ evidence could be observed at the Tevatron, in the mass range up to $M_H = 180$ GeV with 20 fb^{-1}.

In pp collisions at $\sqrt{s} = 14$ TeV, the LHC will produce a light Higgs boson mainly through the loop induced gg-fusion mechanism and, with smaller contribution, from the associated productions WH and $t\bar{t}H$. The ATLAS and CMS experiments have shown that a Higgs boson, with SM couplings, can be discovered over the whole theoretically allowed mass range with convincing significance [7] with an integrated luminosity of 30 fb^{-1}, through the decay modes $\gamma\gamma$ and $b\bar{b}$ for $M_H < 130$ GeV and $ZZ^* \to 4\ell$ for larger masses. For the MSSM Higgs sector, at least one Higgs
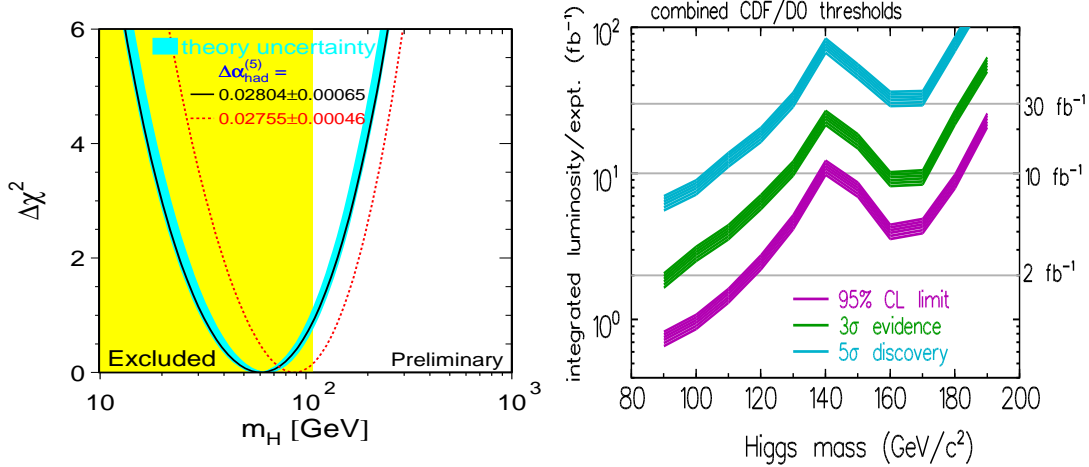
FIGURE 1. Left: χ^2 of the precision electroweak data as a function of the Higgs mass before (thick line) and after (thin line) adding the new BES result [5] in the evaluation of the fine-structure constant α (from [4]). Right: SM Higgs boson discovery potential of Tevatron Run II. The integrated luminosity is per experiment, assuming both experiments are combined (from [6]).

boson can be observed for the entire $M_A - \tan\beta$ parameter space for an integrated luminosity of 300 fb^{-1}.

B   The Linear Collider

At the LC the Higgs boson can be observed in the Higgs-strahlung production process $e^+e^- \rightarrow HZ$ with $Z \rightarrow \ell^+\ell^-$, independently of its decay mode, by a distinctive peak in the di-lepton recoil mass distribution. A data set of 500 fb^{-1} at $\sqrt{s} = 350$ GeV, corresponding to one to three years of LC running with the design parameters of the different projects proposed, provides a sample of 3500-2200 Higgs particles produced in the di-lepton HZ channel, for $M_H = 120$-200 GeV. Taking into account the SM backgrounds, dominated by the $e^+e^- \rightarrow Z^0Z^0$ and W^+W^- productions, the observability of the Higgs boson, at the e^+e^- LC, is guaranteed up to its production kinematical limit, independently of its decay. At a $\gamma\gamma$ LC, a Higgs boson with $M_H < 250$ GeV is produced through $\gamma\gamma \rightarrow H$, with a cross section approximately an order of magnitude larger than that for $e^+e^- \rightarrow HZ$ at the same beam energy. However, the anticipated lower luminosity achievable in $\gamma\gamma$ collisions, the large backgrounds from $\gamma\gamma \rightarrow$ hadrons and the need to analyse predetermined Higgs final states make its detection less efficient and model-dependent.

III   THE STUDY OF THE HIGGS BOSON PROFILE

After the observation of a new particle with properties compatible with those of the Higgs boson, a significant experimental and theoretical effort will be needed to verify that the observed particle is indeed the boson of the scalar field responsible for the electro-weak symmetry breaking and the generation of mass. Outlining the Higgs boson profile, through the determination of its mass, width, quantum numbers, couplings to gauge bosons and fermions and the reconstruction of the Higgs potential, stands as a very challenging physics programme. An e^+e^- LC with its large data sets at different centre-of-mass energies and beam polarisation conditions, the high resolution detectors providing unprecedented accuracy on the event properties and the advanced analysis techniques developed from those adopted at LEP and SLC, promises to promote Higgs physics into the domain of precision measurements.

A   Higgs Mass

Since the Higgs mass M_H is not predicted by theory, it is of great importance to measure it. Once this mass is fixed, the profile of the Higgs particle is uniquely determined in the SM. In theories with extra Higgs doublets, such as SUSY, the measurement of the masses of the physical boson states is important to predict their production and decay properties as a function of the remaining model parameters. At the LC, the Higgs mass can be best measured by exploiting the kinematical characteristics of the Higgs-strahlung production process $e^+e^- \to Z^* \to H^0 Z^0$ where the Z^0 can be reconstructed in both its leptonic and hadronic decay modes. The $\ell^+\ell^-$ recoil mass for leptonic Z^0 decays, yields an accuracy of 110 MeV for
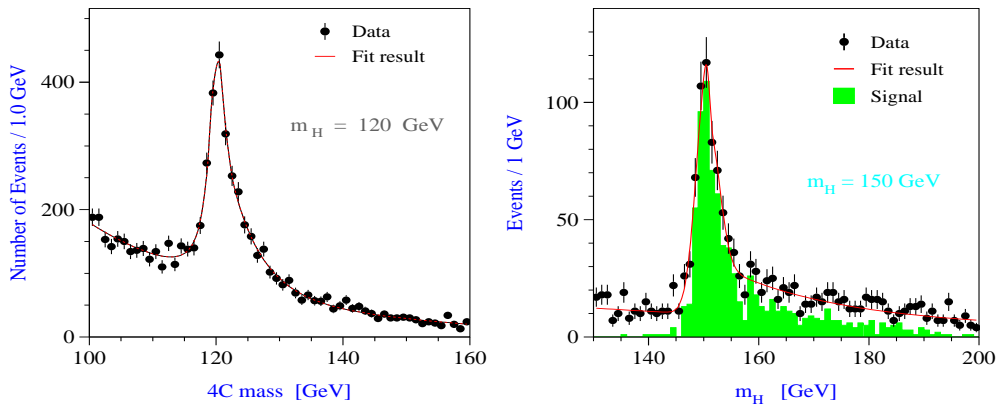

FIGURE 2. The Higgs boson mass reconstructed in the $H^0 \to b\bar{b}$, $Z^0 \to \ell^+\ell^-$ channel for M_H=120 GeV (left) and in the $H^0 \to WW^*$, $Z^0 \to \ell^+\ell^-$ channel for M_H=150 GeV

500 fb^{-1} of data, without any requirement on the nature of the Higgs decays. Further improvement can be obtained by explicitly selecting $H \to b\bar{b}$ (WW) for $M_H \leq (>)$ 140 GeV. Here a kinematical 5-C fit, imposing energy and momentum conservation and the mass of a jet pair to correspond to M_Z, achieves an accuracy of 40 to 90 MeV for 120< M_H < 180 GeV [8].

B   Higgs Quantum Numbers

The spin, parity, and charge-conjugation quantum numbers J^{PC} of the Higgs bosons can be determined at the LC in a model-independent way. This allows a number of general models, involving CP-violating mixture of different Higgs bosons, to be tested. The observation of Higgs production at the photon collider or of the $H \to \gamma\gamma$ decay would rule out $J = 1$ and require C to be positive. The angular dependence of the $e^+e^- \to ZH$ cross-section allows J and P to be determined and can distinguish the SM Higgs boson from a CP-odd 0^{-+} state A, or a CP-violating mixture of the two (generically denoted by Φ in the following). An additional scan of the threshold rise of the Higgs-strahlung cross section can unambiguously verify the scalar nature of the observed state [10]. In a general model with two Higgs doublets (2HDM), the three neutral Higgs bosons correspond to arbitrary mixtures of CP eigenstates, and their production and decay may exhibit CP violation. In this case, the amplitude for the Higgs-strahlung process can be described by adding a ZZA coupling with strength η to the SM matrix element. The squared amplitude for the Higgs-strahlung process $Z \to Z\Phi$ is then given by [9]:

$$|\mathcal{M}|^2 = |\mathcal{M}_{ZH}^{SM}|^2 + \eta 2Re(\mathcal{M}_{ZH}^*\mathcal{M}_{ZA}) + \eta^2|\mathcal{M}_{ZA}|^2 \qquad (1)$$

The first term in $|\mathcal{M}|^2$ corresponds to the SM cross section, the second, linear in η, to the interference term, generates a forward-backward asymmetry resulting in a distinctive signal of CP violation, while the CP-even third term contribution $\eta^2|\mathcal{M}_{ZA}|^2$ increases the total $e^+e^- \to Z\Phi$ cross section. The angular distributions of the accompanying $Z \to f\bar{f}$ decay products are also sensitive to the Higgs CP parity and spin as well as to anomalous couplings. The information carried by these angular distributions has been analysed using the optimal observable formalism for the case of 500 fb^{-1} of e^+e^- data taken at $\sqrt{s} = 350$ GeV for a 120 GeV Higgs boson. The sensitivity to a CP-odd contribution can be determined with a sensitivity of better than 3% [11]. In more generality, for the $ZZ\Phi$ coupling there may be two more independent CP-even terms. Similarly, there may also be an effective $Z\gamma\Phi$ coupling, generated by two CP-even and one CP-odd terms [12] making a total of seven complex couplings, a_Z, b_Z, c_Z, $\tilde{b}_Z$, b_γ, c_γ, and $\tilde{b}_\gamma$, where the tilde denotes the CP-odd couplings, to be probed. With sufficiently high luminosity, accurate τ helicity, good b charge identification and polarisation of both beams it will be possible to determine these couplings from the angular distribution of $e^+e^- \to Z\Phi \to (f\bar{f})\Phi$ as demonstrated by a phenomenological analysis [12].
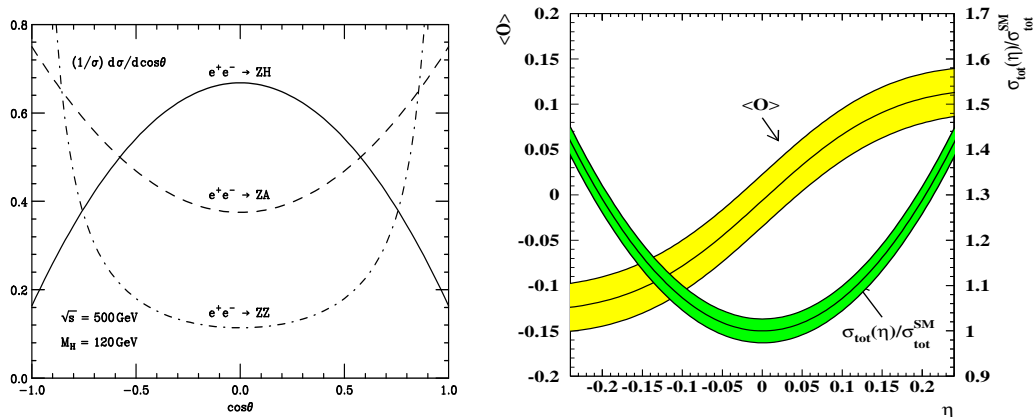
FIGURE 3. The $\cos\theta$ dependence of $e^+e^- \rightarrow ZH$, $e^+e^- \rightarrow ZA$, $e^+e^- \rightarrow ZZ$ for $\sqrt{s} = 500$ GeV, assuming a Higgs boson mass of 120 GeV [16] (left) and the dependence of the expectation value of the optimal observable and the total cross section on η for $M_H = 120$ GeV, $\sqrt{s} = 350$ GeV and $\mathcal{L} = 500\ fb^{-1}$ after applying the selection cuts and detector simulation. The shaded bands show the $1 - \sigma$ uncertainty in the determination of $< \mathcal{O} >$ and $\sigma_{Z\Phi}$.

C   Higgs Couplings to Fermions

The SM Higgs couplings to fermion pairs $g_{Hff} = m_f/v$ are fully determined by the fermion mass m_f. The corresponding decay partial widths only depend on these couplings and on the Higgs mass. Therefore, their accurate determination will represent a comprehensive test of the Higgs mechanism in the SM. Further, observing deviations of the measured values from the SM predictions probes the parameters of an extended Higgs sector. The accuracy of these measurements relies on the performances of the jet flavour tagging algorithms and thus on those of the Vertex Tracker, making this analysis a major benchmark for optimising the detector design. Several analyses have been performed [13–15]. The measurement of the decays into $b\bar{b}$, $c\bar{c}$, gg and $\tau^+\tau^-$ is based on the selection of Higgs decays into two fermions in the $jjjj$, $jj\ell\ell$ and $jj + E_{miss}$ topologies. The decay rates for the individual hadronic modes are extracted by a likelihood fit to the jet flavour tagging response, while the τ final states are selected by a dedicated likelihood, based on vertexing and calorimetric response to separate the $H \rightarrow \tau^+\tau^-$ from the hadronic decays. For $M_H \leq 140$ GeV, the hadronic modes have branching fractions that are large enough in the SM to be measured to an accuracy better or comparable to their theoretical uncertainties. For larger values of the Higgs boson mass, as the WW^* decay becomes predominant, the $H \rightarrow b\bar{b}$ decay can still be measured with an accuracy better than 10% up to 170 GeV.

The Higgs coupling to the top quark, is the largest coupling in the SM ($g_{Htt}^2 \simeq 0.5$ to be compared with $g_{Hbb}^2 \simeq 4 \times 10^{-4}$). However, for a light Higgs boson this
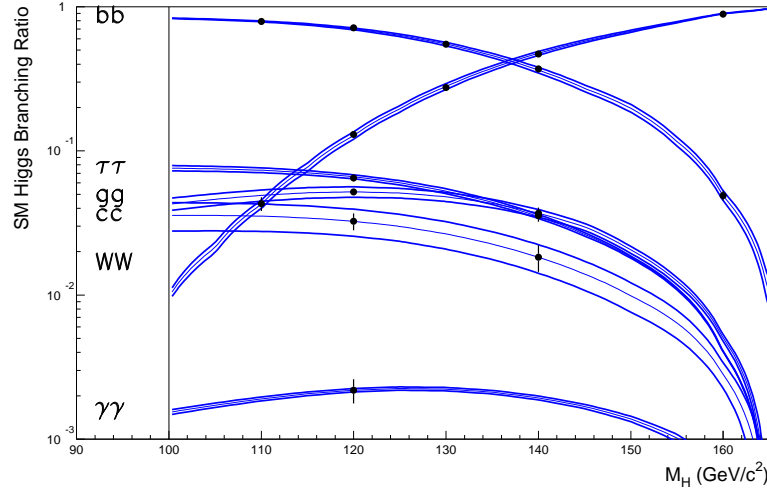
FIGURE 4. SM predictions for the Higgs boson decay branching ratios as a function of M_H. Points with error bars show the expected experimental accuracy, while the lines show the estimated uncertainties on the SM predictions due to the value of the fermion masses and of α_s.

coupling is accessible indirectly in the loop process $H \to gg$ and directly only in the Yukawa process $e^+e^- \to t\bar{t}H$ [17]. This process has a cross section of the order of only 0.5 fb for $M_H \sim 120$ GeV at $\sqrt{s} = 500$ GeV and 2.5 fb at $\sqrt{s} = 800$ GeV. The QCD corrections have been calculated recently up to next-to-leading order [18] and were found to be large and positive at $\sqrt{s} \sim 500$ GeV because of threshold effects, while they become small and negative at $\sqrt{s} \sim 1$ TeV. The distinctive signature, consisting of two W bosons and four b-quark jets, makes it possible to isolate these events from the thousand times larger backgrounds. In consideration of the small statistics, the analysis uses a set of highly efficient pre-selection criteria and a Neural Network trained to separate the signal from the remaining backgrounds. Because the backgrounds are so large, it is crucial that they should be well modelled both in absolute level and in the event shapes which

TABLE 1. Relative accuracy in the determination of Higgs boson decay branching ratios for 500 fb^{-1} at $\sqrt{s} = 350$ GeV

Channel	$M_H = 120$ GeV	$M_H = 140$ GeV	$M_H = 160$ GeV
$H^0/h^0 \to b\bar{b}$	$\pm$ 0.024	$\pm$ 0.026	$\pm$ 0.065
$H^0/h^0 \to c\bar{c}$	$\pm$ 0.085	$\pm$ 0.190	
$H^0/h^0 \to gg$	$\pm$ 0.055	$\pm$ 0.140	
$H^0/h^0 \to \tau^+\tau^-$	$\pm$ 0.050	$\pm$ 0.080	

determine how they are treated by the Neural Net. For an integrated luminosity of 1000 fb^{-1} at $\sqrt{s} = 800$ GeV, the uncertainty in the Higgs-top Yukawa coupling after combining the semileptonic and the hadronic channels is $\pm$ 4.2% (stat), for $M_H = 120$ GeV, becoming $\pm$ 5.5% (stat+syst) by assuming a 5% uncertainty in the overall background normalisation [19].

If the Higgs boson mass is larger than the kinematical threshold for $t\bar{t}$ production, the Higgs Top Yukawa couplings can be measured from the $H \rightarrow t\bar{t}$ branching fractions, similarly to those of the other fermions discussed previously in this section. A study has been performed based on the analysis of the process $e^+e^- \rightarrow \nu_e\bar{\nu}_e H \rightarrow \nu_e\bar{\nu}_e t\bar{t}$ for 350 GeV$< M_H <$ 500 GeV at $\sqrt{s} = 800$ GeV. The $e^+e^- \rightarrow t\bar{t}$ and the $e^+e^- \rightarrow e^+e^- t\bar{t}$ backgrounds are reduced by an event selection based on the characteristic event signature with six jets, two of them from a b quark, on the missing energy and the mass. Since the S/B ratio is expected to be large, the uncertainty on the top Yukawa coupling is dominated by the statistics and corresponds to 7% (15%) for $M_H = 400$ (500) GeV for an integrated luminosity of 500 fb^{-1} [20].

D   Higgs Couplings to Massive Gauge Bosons

In the SM the coupling of the Higgs boson to the massive gauge bosons is given by $g_{HVV} = 2M_V^2/v$ for $V = W, Z$. The ratio of the $W^\pm$ and Z^0 couplings is dictated by the $SU(2) \times U(1)$ symmetry and thus valid in any model obeying this experimentally well established symmetry.

At the LC, both couplings can be probed independently with high accuracy. The g_{HZZ} coupling is most sensitively probed through the measurement of the cross section for the Higgs–strahlung process, $e^+e^- \rightarrow H^0 Z^0$, which at tree level is proportional to g_{HZZ}^2. Since the recoil mass method allows to extract this cross section independently of the subsequent Higgs boson decay, no further model assumptions need to be made. Detailed experimental studies have shown that the Higgs–strahlung cross section can be measured with accuracies between 2.4% and 3.0% for Higgs boson masses between 120 and 160 GeV [8] only deteriorating slowly for higher Higgs boson masses due to the decreasing production cross section.

The g_{HWW} coupling is probed both through the measurement of the cross section for the WW–fusion process and the decay branching ratio for $H^0 \rightarrow WW^*$. The WW–fusion cross section has been studied in the $\nu\bar{\nu}b\bar{b}$ final state for $M_H \leq$ 160 GeV. The contributions to this final state from WW-fusion, Higgs–strahlung with $Z^0 \rightarrow \nu\bar{\nu}$ and the remaining four–fermion final states can be separated, exploiting their different characteristics in the spectrum of the $\nu\bar{\nu}$ invariant mass, which is measurable through the missing mass distribution. From a simultaneous fit to these contributions the WW–fusion cross section can be extracted with accuracies between 2.8% and 13% for Higgs boson masses between 120 and 160 GeV [21]. The different behaviour of the contributions to the missing mass spectrum for different polarisations of the e^+ and the e^- beam is advantageous to control systematic un-

TABLE 2. Relative accuracy on the determination of the Higgs production cross sections and decay branching ratios in gauge bosons for 500 fb^{-1} of LC data at $\sqrt{s}$ = 350 or 500 GeV.

	$\delta\sigma/\sigma$ M_H=120 GeV	$\delta\sigma/\sigma$ M_H=140 GeV	$\delta\sigma/\sigma$ M_H=160 GeV
$\sigma(e^+e^- \to HZ)$	±0.024	±0.027	±0.030
$\sigma(e^+e^- \to H\nu_e\bar{\nu}_e)$	±0.028	±0.037	±0.130
BR($H \to WW^*$)	±0.051	±0.025	±0.021

certainties. The possibility to exploit the $\nu\bar{\nu}WW^*$ and $\nu\bar{\nu}ZZ^*$ final states at higher values of M_H is promising to extend the mass reach of this measurement but has not yet been studied in detail.

The measurement of the branching ratio $H \to WW^*$ provides an alternative means to access the g_{HWW} coupling. This branching ratio can be measured in Higgs–strahlung events and has been studied in the $Z \to \ell^+\ell^-, H \to q\bar{q}'q\bar{q}'$ and $Z \to q\bar{q}, H \to q\bar{q}'\ell\nu$ channels [22]. The analyses take advantage of the excellent jet-jet invariant mass resolution achievable for future LC detectors under study. The achievable precision is 5.1% to 2.1% for Higgs boson masses between 120 and 160 GeV.
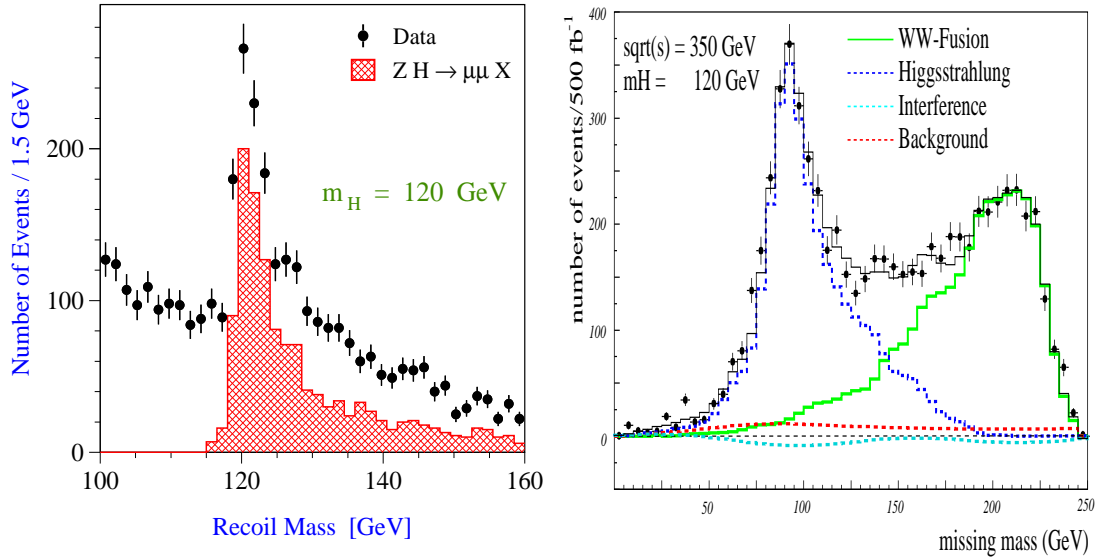

FIGURE 5. Observables for the Higgs couplings to the Z^0 and $W^\pm$ gauge bosons. Left: di-lepton recoil mass in the Higgs-strahlung process $e^+e^- \to HZ \to X\ell^+\ell^-$. Right: missing mass distribution in $b\bar{b}\nu\bar{\nu}$ events. The WW fusion contribution to the Higgs production is measured from a fit to the shape of this distribution.

E Higgs Coupling to Photons

The Higgs effective coupling to photons is mediated by loops, dominated in the SM by the W contribution but also sensitive to any massive charged particles coupling directly to the Higgs and to the photons. In the case of enhanced Hbb or Htt couplings or contributions from charged Higgs bosons, the $\gamma\gamma$ effective couplings may deviate significantly from its SM prediction and provides insight into the structure of the Higgs sector [23]. This coupling can be tested both through the $\gamma\gamma \to H$ production at a $\gamma\gamma$ collider and the Higgs decay channel $H \to \gamma\gamma$. The $\gamma\gamma \to H$ cross section being very substantial, a light Higgs can be observed through its $b\bar{b}$ decay provided an effective suppression of the large $\gamma\gamma \to c\bar{c}$ background is achieved. With an integrated luminosity of 150 fb^{-1}, an accuracy of 2% on $\sigma(\gamma\gamma \to H)$ can be achieved for a 120 GeV SM-like Higgs [24]. The corresponding decay branching fraction can be measured in both the $\nu\bar{\nu}\gamma\gamma$ and $\gamma\gamma+$jets final states. The $e^+e^- \to Z\gamma\gamma$ double bremsstrahlung process represents the most important background process. This can be reduced by exploiting the photon energy and angular distributions. Since the SM prediction for BR$(H \to \gamma\gamma)$ is only 2×10^{-3}, it can only be measured with an accuracy of 19% for 500 fb^{-1} of data. The error is reduced to 13% for 1000 fb^{-1} [25].

F Extraction of Higgs Couplings

The Higgs boson production and decay rates discussed above, can be used to measure the Higgs couplings to gauge bosons and fermions. Since some of the couplings of interest can be determined independently by different observables while other determinations are partially correlated, it is interesting to perform a global fit to the measurable observables to extract the Higgs couplings. This method makes optimal use of the available information and can take properly into account the correlation originating from the experimental techniques.

TABLE 3. Relative accuracy on Higgs couplings for 500 fb^{-1} of LC data

Coupling	$M_H = 120$ GeV
g_{HWW}	$\pm$ 0.012
g_{HZZ}	$\pm$ 0.012
g_{Htt}	$\pm$ 0.022
g_{Hbb}	$\pm$ 0.021
g_{Hcc}	$\pm$ 0.031
$g_{H\tau\tau}$	$\pm$ 0.032

A dedicated program, HFITTER [26] has been developed based on the HDECAY [27] program for the calculation of the Higgs boson branching ratios. The
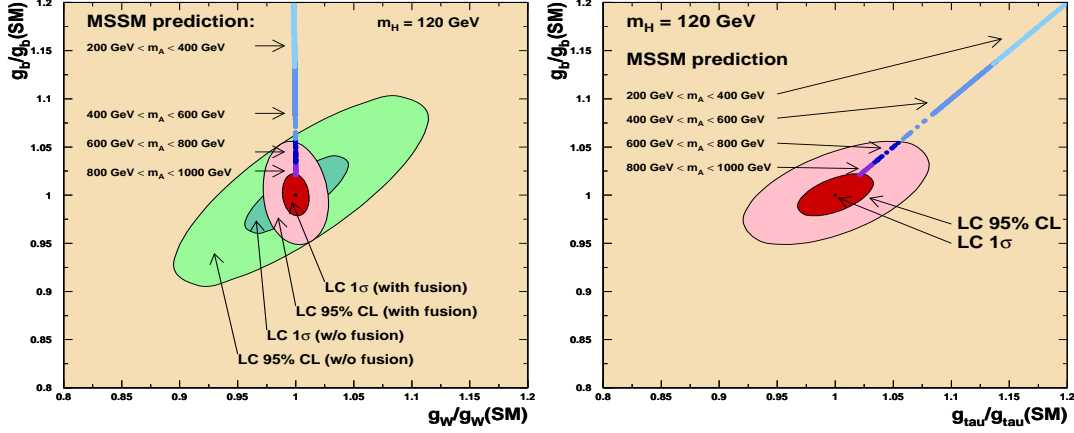
FIGURE 6. Higgs coupling determinations at the LC. The contours for the g_{Hbb} vs. g_{HWW} (left) and g_{Hbb} vs. $g_{H\tau\tau}$ (left) couplings for a 120 GeV Higgs boson as measured with 500 fb^{-1} of data.

following inputs have been used: σ_{HZ}, $\sigma_{H\nu\bar{\nu}}$, BR($H \to WW$), BR($H \to \gamma\gamma$), BR($H \to b\bar{b}$), BR($H \to \tau^+\tau^-$), BR($H \to c\bar{c}$), BR($H \to gg$), $\sigma_{t\bar{t}H}$. For correlated measurements the full covariance matrix has been used. The results are given for $M_H = 120$ GeV and 500 fb^{-1}. Table 3 shows the accuracy which can be achieved in determining the couplings.

G   Higgs Boson Width

The total decay width of the Higgs boson is predicted to be too narrow to be resolved experimentally for Higgs boson masses below the ZZ–threshold. Above approximately 200 GeV the total width can be measured directly from the reconstructed width of the recoil mass peak.

For lower masses, indirect methods, exploiting relations between the total decay width and the partial widths for exclusive final states, must be applied. In general, the total width is given by $\Gamma_{tot} = \Gamma_X / \text{BR}(H \to X)$. Thus whenever Γ_X can be determined independently of the corresponding branching ratio, a measurement of Γ_{tot} can be carried out. Two feasible options exist for light Higgs bosons: i) the extraction of Γ_{WW} from the measurement of the WW–fusion cross section combined with the measurement of BR(H $\to$ WW*) and ii) the measurement of the $\gamma\gamma \to H$ cross section at a $\gamma\gamma$ collider combined with the measurement of BR(H $\to \gamma\gamma$) in e^+e^- collisions. The WW–fusion option yields a precision of 6% to 13% for Higgs boson masses between 120 and 160 GeV, while the $\gamma\gamma$ option yields a larger error dominated by the large uncertainty in the BR(H $\to \gamma\gamma$) determination discussed above.

Assuming the $SU(2) \times U(1)$ relation $g^2_{HWW}/g^2_{HZZ} = 1/\cos^2\theta_W$ to be valid, the

measurement of the Higgs–strahlung cross section provides a viable alternative with potentially higher mass reach than the WW–fusion option.

H   Higgs Potential

The observation of the scaling of the Higgs couplings to fermions with their mass will provide with a proof that the interaction with the Higgs field is responsible for the mass generation. However, in order to fully establish the Higgs mechanism, the Higgs potential $V = \lambda \ (|\phi|^2 - \frac{1}{2}v^2)^2$ with $v = (\sqrt{2}G_F)^{-1/2} \simeq 246$ GeV must be reconstructed through the determination of the triple, λ_{HHH}, and quartic, λ_{HHHH}, Higgs self couplings. While effects from the quartic coupling may be too small to be observed at the LC, the triple Higgs coupling can be measured in the double Higgs boson production processes $e^+e^- \rightarrow HHZ$ and $\nu_e\bar{\nu}_eHH$. In e^+e^- collisions up to 1 TeV the double Higgs boson associated production with the Z is favoured, while at a multi-TeV collider the $\nu_e\bar{\nu}_eHH$ reaction becomes dominant [28]. The sensitivity
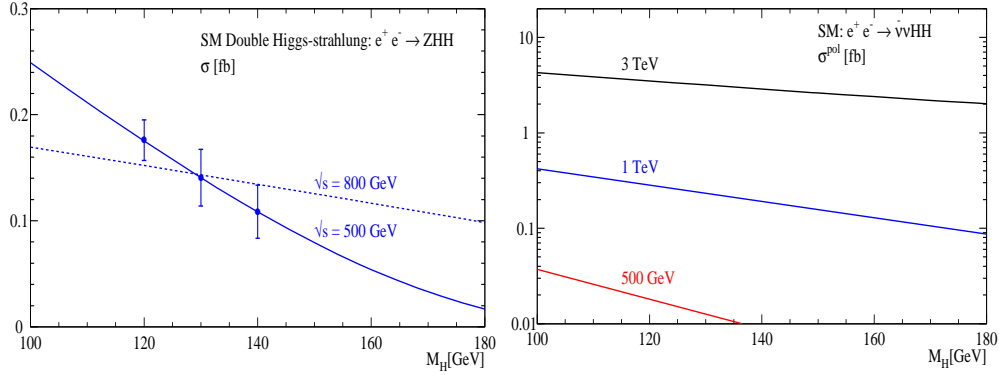

FIGURE 7. Cross sections sensitive to the triple Higgs coupling. $\sigma(e^+e^- \rightarrow HHZ)$ (left) and $\sigma(HH\nu\bar{\nu})$ (right) as a function of M_H for different LC centre-of-mass energies.

to λ_{HHH} from the measurement of σ_{HHZ} and $\sigma_{\nu\bar{\nu}HH}$ is diluted by the effects of other diagrams, not involving the triple Higgs coupling but leading to the same final state. The four and six fermion backgrounds and the small signal cross section make this measurement an experimental challenge . The distinctive 4 b-jet signature and the $M_{b\bar{b}} = M_H$ constraints allow to reduce these backgrounds to get $S/\sqrt{B} \simeq 6$ with 1000 fb^{-1} of data collected at $\sqrt{s} = 500$ GeV, provided a performant b-tagging and energy flow response of the detector [29]. This corresponds to a determination of λ_{HHH} with a statistical accuracy of 22% for $M_H = 120$ GeV with 1000 fb^{-1}. A second phase LC, delivering multi-TeV e^+e^- collisions, could improve this accuracy to better than 10%.

In the SM extensions with an extra Higgs doublet, additional trilinear Higgs couplings are also present such as λ_{hhH}, λ_{hhA}, λ_{hhh} and λ_{HAA}. While these depend also on the $\tan\beta$ and M_A parameters, the topologies analysed for the case of the SM also apply to that of the λ_{hhh} except for the limited region of parameters where

the $h \to b\bar{b}$ decay is suppressed. The corresponding analysis can be repeated for trilinear Higgs couplings in the supersymmetric extension of the Standard Model. The sensitive area in the $[M_A, \tan\beta]$ plane depends on the states that can be analysed as described in detail in [30].

IV   HIGGS BOSONS IN SUPERSYMMETRY

Several extensions of the SM introduce additional Higgs doublets. In the simplest of such extensions (2HDM), the Higgs sector consists of two doublets generating five physical Higgs states: h^0, H^0, A^0 and $H^\pm$. The h^0 and H^0 states are CP even and the A is CP odd. Besides the masses, two mixing angles define the properties of the Higgs bosons and their interactions with gauge bosons and fermions defined through the ratio of the vacuum expectation values $v_2/v_1 = \tan\beta$ and a mixing angle α in the neutral CP-even sector. Two Higgs doublets naturally arise in the context of the minimal supersymmetric extension of the SM (MSSM). The study of the lightest neutral MSSM Higgs boson h^0 follows closely that of the SM H discussed above and those results remain in general valid. The ability of the LC to tell the SM/MSSM nature of a neutral Higgs, based solely on its properties, is discussed in the next section. In SUSY models, additional decay channels may open for the h^0 boson, if there are light enough SUSY particles. The most interesting scenario is that in which the Higgs decays in particles escaping detection, such as $h^0 \to \chi^0\chi^0$, giving a sizeable $H \to$ invisible decay width. While the Higgs observability in the dilepton recoil mass in the associated HZ production channel is virtually unaffected by this scenario, such an invisible decay width can be measured by comparing the number of $e^+e^- \to ZH \to \ell^+\ell^-$ anything events with the sum over the visible decay modes corrected by the $Z^0 \to \ell^+\ell^-$ branching fraction: BR($Z \to \ell^+\ell^-$) $\times (\sum_{i=b,c,\tau,...} N_{ZH \to f_i\bar{f}_i} + \sum_{j=W,Z,\gamma} N_{ZH \to B_j\bar{B}_j})$. By taking the accuracies on the determination of the individual branching fractions discussed above, the rate for the $H \to$ invisible decay can be determined to better than 20% for BR($H \to$ invisible)>0.05.

A   Tell the SM from a MSSM Neutral Higgs

The discovery of a neutral Higgs boson, with mass in the range 115 GeV $< M_H <$ 140 GeV, will raise the question of whether the observed particle is the SM Higgs boson or the lightest boson from the Higgs sector of a SM extension. It has been shown that, for a large fraction of the $\tan\beta - M_A$ parameter plane in the MSSM, this neutral boson will be the only Higgs state observed at the LHC (see Figure 10). It is possible, that the scale M_{SUSY} is high and the supersymmetric fermion partners may not be visible at a 500 GeV linear collider. In this circumstance, a Higgs particle generated by a complex multi-doublet model could be indirectly recognised only by a study of its couplings. If the HZZ coupling, measured by the

Higgs-strahlung production cross-section independently from the Higgs boson decay mode, turns out to be significantly smaller than the SM expectation, this will signal the existence of extra Higgs doublets.

The determination of the Higgs boson decay branching ratios with the accuracy anticipated by these studies can be employed to identify the SM or MSSM nature of a light neutral Higgs boson. The Higgs boson decay widths Γ^{MSSM} to a specific final state are modified as follows with respect to the SM Γ^{SM}: $\Gamma_{b\bar{b}}^{MSSM} \propto \Gamma_{b\bar{b}}^{SM} \frac{\sin^2 \alpha}{\cos^2 \beta}$ and $\Gamma_{c\bar{c}}^{MSSM} \propto \Gamma_{c\bar{c}}^{SM} \frac{\cos^2 \alpha}{\sin^2 \beta}$. Therefore, deviations in the ratios of branching ratios such as $\frac{BR(h \rightarrow WW^*)}{BR(h \rightarrow bb)}$, $\frac{BR(h \rightarrow c\bar{c})}{BR(h \rightarrow bb)}$ and $\frac{BR(h \rightarrow gg)}{BR(h \rightarrow bb)}$ from their SM expectations can reveal the MSSM nature of the Higgs boson and also provide indirect information on the mass of the CP-odd A^0 Higgs boson, even when it is so heavy that it can not be directly observed at $\sqrt{s} = 500$ GeV.

To compare the SM predictions with those in MSSM, a complete scan of the MSSM parameter space has been performed. For each set of parameters, the h^0 mass has been computed using the diagrammatic two-loop result [31]. Solutions corresponding to $M_{h^0} = (120 \pm 2)$ GeV have been selected and used to compute the h^0 decay branching ratios accounting for squark loops [27]. The deviations from the SM predictions for $\mathrm{BR}(h \rightarrow b\bar{b})/\mathrm{BR}(h \rightarrow \text{hadrons})$, $\mathrm{BR}(h \rightarrow c\bar{c})/\mathrm{BR}(h \rightarrow \text{hadrons})$, $\mathrm{BR}(h \rightarrow gg)/\mathrm{BR}(h \rightarrow \text{hadrons})$ and $\mathrm{BR}(h \rightarrow b\bar{b})/\mathrm{BR}(h \rightarrow WW^*)$ have been used to investigate the SM/MSSM discrimination. Figure 8 shows the region of the $M_A - \tan\beta$ plane in which there are more than 68%, 90% or 95% of the MSSM solutions outside the SM 95% confidence level region defined by the total χ^2 probability for the observed branching ratios.
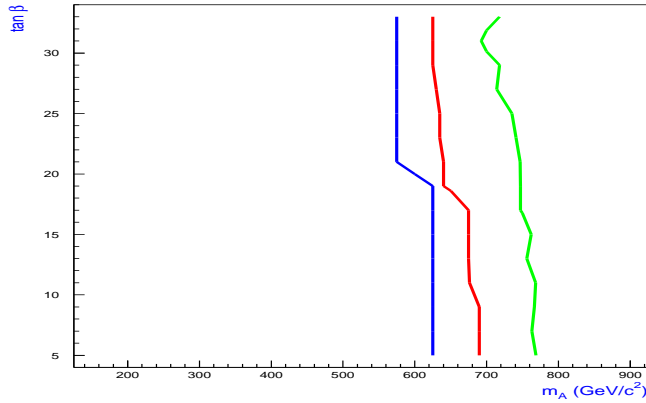

FIGURE 8. Sensitivity to SM/MSSM Higgs boson nature as a function of M_A and $\tan\beta$ from determinations of h^0 BRs at the LC with 1000 fb^{-1}. The curves show the upper bound of the regions with 68%, 90% and 95% (from right to left) of the MSSM solutions distinguishable from the SM branching fraction predictions.

If a significant indication of MSSM has been observed, which implies that M_A is

within the limit of Figure 8, then it is possible to go further and use the accurate measurements of the Higgs boson decays to obtain an indirect estimate of the mass M_{A^0}. The sensitivity to the A^0 mass arises from the MSSM corrections to the Higgs couplings discussed above and it is of special interests for those masses above the kinematical limit for direct $e^+e^- \to h^0 A^0$, $H^0 A^0$ production. The analysis has been performed assuming given sets of measured values for the $\mathrm{BR}(h \to c\bar{c})/\mathrm{BR}(h \to b\bar{b})$, $\mathrm{BR}(h \to g\bar{g})/\mathrm{BR}(h \to b\bar{b})$ and $\mathrm{BR}(h \to WW^*)/\mathrm{BR}(h \to b\bar{b})$ ratios. The A^0 mass has been varied together with the other MSSM parameters within the range compatible with the measured branching ratios allowing for their total uncertainty. The range of values of M_A for the accepted MSSM solutions corresponds to an accuracy of 70 GeV to 100 GeV for the indirect determination of M_A in the mass range 300 GeV $< M_A <$ 600 GeV.

B   Properties of the Heavy Higgs Sector

A most distinctive feature of extended models such as supersymmetry, or general 2HDM extensions of the SM, is the existence of additional Higgs bosons. Their mass and coupling patterns vary with the model parameters. However in the decoupling limit, the $H^\pm$, H^0 and A^0 bosons are expected to be heavy and to decay predominantly into quarks of the third generation.
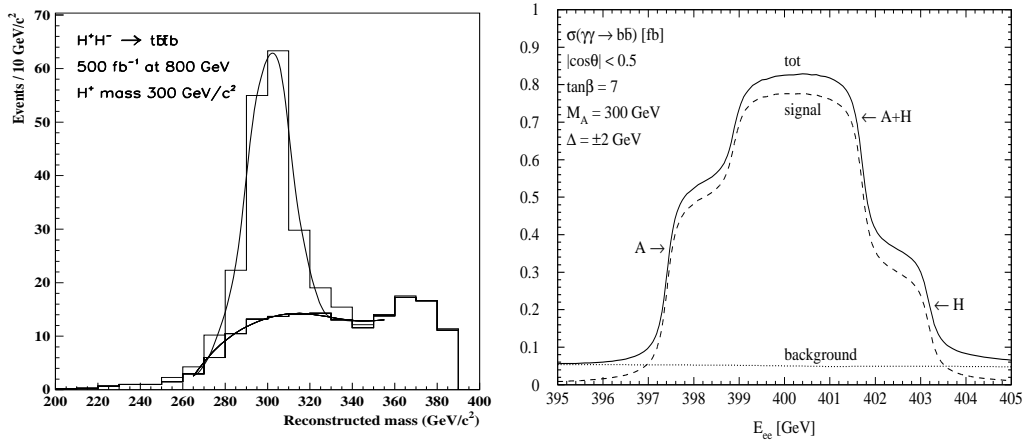

FIGURE 9. Examples of the signals from 300 GeV SUSY Higgs bosons at the LC for e^+e^- and $\gamma\gamma$ collisions. Left: Di-jet invariant mass distribution for $e^+e^- \to H^+H^- \to t\bar{b}\bar{t}b$ charged Higgs boson events after intermediate W and t mass and equal mass final state constraints. Right: Scan of the $\gamma\gamma \to A^0$ and H^0 thresholds showing the sensitivity to the small mass splitting of nearly degenerate A^0 and H^0 Higgs bosons.

Establishing their existence and the determination of their mass and main decay modes, through their pair production $e^+e^- \to H^0 A^0$, H^+H^- will represent an important part of the LC physics programme at $\sqrt{s} \geq 500$ GeV. The decay channels

H^0, $A^0 \to b\bar{b}$, $H^+ \to t\bar{b}$ or W^+h^0, $h^0 \to b\bar{b}$ will provide with very distinctive 4 jet and 8 jet final states with 4 b-quark jets that can be efficiently identified and reconstructed. Exemplificative analyses have been performed for these channels, showing that an accuracy of about 0.3% on their mass and of $\simeq 10\%$ on $\sigma \times BR$ can be obtained [32,33]. In addition, $\gamma\gamma \to H^+H^-$ pair production and $\gamma\gamma \to A^0$ and H^0 at the $\gamma\gamma$ collider, is characterised by sizable cross sections and may also probe the heavier part of the Higgs spectrum in SM extensions. In particular, a scan of the A^0 and H^0 thresholds at the $\gamma\gamma$ collider can resolve a small $A^0 - H^0$ mass splitting [34] (see Figure 9). A detailed analysis of their production and decay, using polarised colliding photons, provides an opportunity to determine the quantum numbers of the heavy bosons and therefore to distinguish the A^0 from the H^0 boson [35].

V   THE LC, THE LHC AND THE FMC

While the LC offers an accurate and comprehensive test of the Higgs sector properties, the LHC pp collider, under construction at CERN, will independently probe the Higgs sector of the SM and its extensions and a muon collider, through the s-channel Higgs production, also has a claim to the precision study of a light Higgs boson. We summarise here the main arguments on the complementary role of the LC compared to the Higgs boson picture that may be obtained on the basis of the LHC data, as anticipated by the present studies, and compare the LC reach to that of a muon collider.

At the LHC the SM Higgs boson, or at least one Higgs boson in SUSY extensions, will be observed, unless it decays invisibly, as discussed above, while scenarios with extended Higgs sectors or non standard Higgs decay modes have been proposed that may evade the LHC probe of the existence of a Higgs boson. Beyond discovery, measuring the Higgs properties in pp collisions is difficult due to the limited signal statistics, large backgrounds and systematic uncertainties arising, for example from the limited precision of the parton densities in the proton. Still, the LHC data can provide ratios of some of the Higgs branching ratios and couplings, as listed in Table 4 for $M_H = 120$ GeV, while the precision measurements of the absolute branching ratios and couplings remain an experimental program which can only be addressed at a high luminosity lepton collider.

Further perspectives for measurements of the total Higgs boson width and of the g_{HWW} coupling with a precision of 10–20% have been recently suggested for the LHC [36] but are still awaiting to be confirmed experimentally, accounting for the backgrounds and the detector response. Since over a large range of the parameter space, only one Higgs boson is observable at the LHC, the distinction of the SM or SUSY nature of the Higgs sector can only be addressed at a lepton collider, while the LHC may discover supersymmetry by directly observing sparticle decays.

The complementarity of the linear collider data to the picture of the Higgs sector as it will have been outlined by the LHC is therefore threefold: i) the accuracy of
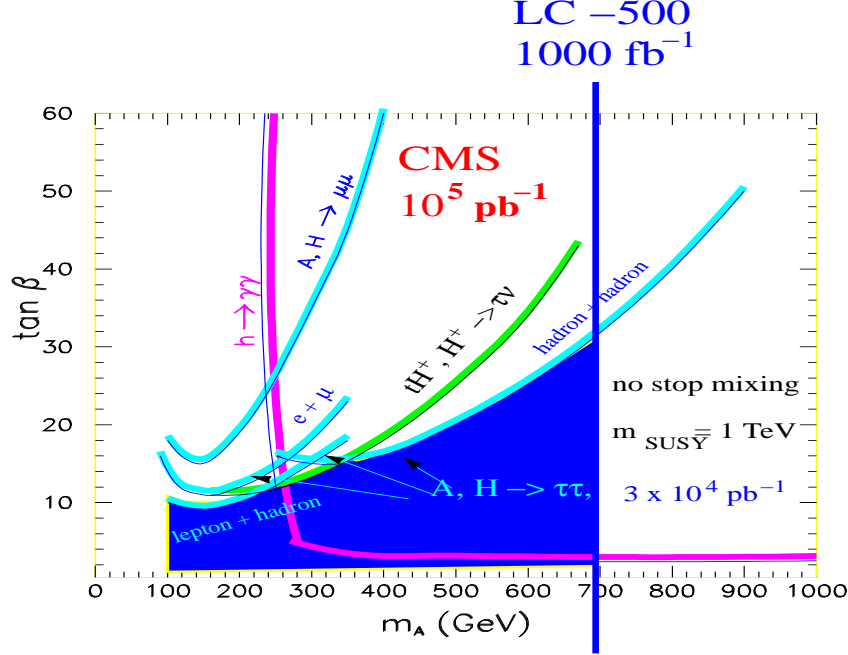
FIGURE 10. Comparison of the MSSM Higgs sector discovery potential at the LHC and at the LC. The LHC data, from the CMS experiment simulation, show the portions of the M_A - $\tan\beta$ plane where the extended nature of the Higgs sector can be established by the observation of additional Higgs bosons. The accurate measurement of the lightest Higgs boson couplings at the LC for $\sqrt{s} = 500$ GeV allows to complement this information by revealing the Higgs boson nature in the dark shaded region, for M_A up to $\simeq 700$ GeV.

those measurements, which are possible at the LHC, can be significantly increased, ii) the absolute measurements of all the relevant Higgs boson couplings, including the Higgs self coupling, will be possible only at the lepton collider and iii) extended Higgs sector scenarios (e.g. invisible Higgs boson decays or 2HDM) can be observed at the linear collider closing the loopholes of a possible non-discovery at the LHC.

If the considerable technical challenges presented by a muon collider project can be properly addressed, a first muon collider (FMC) [37,38] could be operated at the centre-of-mass energy corresponding to a light Higgs boson mass. Such a machine would provide with the unique feature of s-channel $\mu^+\mu^- \to H$ production with a beam energy spread comparable to the natural width of a light SM Higgs boson. However such a small energy spread may only be achieved at a luminosity of about 10^{31} cm^{-1}s^{-1}, corresponding to the production of a few thousand Higgs particles/year. By an energy scan of the Higgs resonance, the FMC can determine its mass and width to an accuracy of better than 1 MeV. The measurement of the $\mu^+\mu^- \to H \to b\bar{b}$ cross section would offer sensitivity to the Higgs couplings to the b quark. This measurement can thus be used, together with those of the Higgs width and mass for a test the Higgs boson nature, similarly to that discussed above for the case of the e^+e^- collider. A comparable sensitivity to the MSSM

TABLE 4. Summary of the Higgs boson profile from the LHC and the LC data. Relative accuracies for the measurement of Higgs properties for different Higgs boson masses.

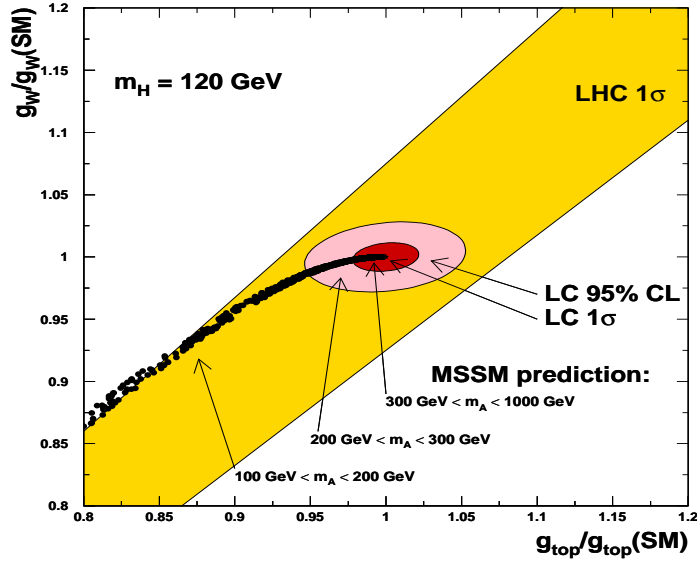|	M_H (GeV/c^2)	$\delta(X)/X$ LHC $2 \times 300\ \mathrm{fb}^{-1}$	$\delta(X)/X$ LC $500\ \mathrm{fb}^{-1}$
M_H	120	9×10^{-4}	3×10^{-4}
M_H	160	10×10^{-4}	4×10^{-4}
$\frac{g_{Htt}}{g_{HWW}}$	120	0.070	0.023
$\frac{g_{HZZ}}{g_{HWW}}$	160	0.050	0.022
Γ_{tot}	120-140	-	0.04 - 0.06
g_{Huu}	120-140	-	0.02 - 0.04
g_{Hdd}	120-140	-	0.01 - 0.02
g_{HWW}	120-140	-	0.01 - 0.03
$\Phi = H + A$	120-140	-	0.03 - 0.13
λ_{HHH}	120	-	0.22

FIGURE 11. Accuracy in the determination of the g_{Htt} and g_{HWW} Higgs boson couplings at the LHC and at the LC compared to the predictions from MSSM for different values of the M_A mass.

Higgs nature can be obtained with 200 pb^{-1}, while a significant extension towards larger values of M_A would require an order of magnitude higher luminosity [38]. Considering the different maturity of the LC and FMC projects, the LC appears

at present as the most attractive option for a detailed investigation of the Higgs sector, complementing the data from the Tevatron and the LHC, at the turn of the first decade of this new century.

VI SUMMARY

The search for the Higgs boson and the study of its properties is one of the main goals of present research in particle physics. The central role of a linear collider in the understanding of the mechanism of electro-weak symmetry breaking, complementing the data delivered by LEP and those to be acquired at the Tevatron and at the LHC, has been clearly outlined by the studies carried out world-wide, reported at this Conference and summarised in this review.

ACKNOWLEDGEMENTS

REFERENCES

1. P.W. Higgs, *Phys. Rev. Lett.* **12** (1964) 132; *idem*, *Phys. Rev.* **145** (1966) 1156; F. Englert and R. Brout, *Phys. Rev. Lett.* **13** (1964) 321; G.S. Guralnik, C.R. Hagen and T.W. Kibble, *Phys. Rev. Lett.* **13** (1964) 585.

2. A. Hasenfratz *et al.*, *Phys. Lett.* **B199** (1987) 531; M. Lüscher and P. Weisz, *Phys. Lett.* **B212** (1988) 472; M. Göckeler *et al.*, *Nucl. Phys.* **B404** (1993) 517.

3. P. Igo-Kemenes for the LEP Higgs working group, talk given at the open session of the LEPC comittee, CERN, Nov 2000; see also: R. Barate *et al.* (ALEPH Coll.), *Phys. Lett.* **B495** (2000) 1; M. Acciari *et al.* (L3 Coll.), *Phys. Lett.* **B495** (2000) 18.

4. The LEP Collaborations, *A Combination of Preliminary Electroweak Measurements and Constraints on the Standard Model*, CERN-EP Note in preparation.

5. Z.G. Zhao (BES Coll.), to appear in the proceedings of the XXXth *Int. Conf. on High Energy Physics*, Osaka, July 2000 and hep-ex/0012038.

6. M. Carena *et. al.*, *Report of the Tevatron Higgs working group*, hep-ph/0010338.

7. A. Caner, to appear in the proceedings of the XXXth *Int. Conf. on High Energy Physics*, Osaka, July 2000.

8. P.G. Abia, these proceedings.

9. A. Djouadi and B.A. Kniehl, DESY 93-123C, 51.

10. D. Miller, these proceedings.

11. M. Schumacher, LC-PHSM-2001-003.

12. K. Hagiwara *et al.*, *Eur. Phys. J.* **C14** (2000) 457 and J. Kamoshita, these proceedings.
13. M.D. Hildreth, T.L. Barklow and D.L. Burke, *Phys. Rev. Lett.* **49** (1994), 3441.
14. M. Battaglia, in Proc. of the *Worldwide Study on Physics and Experiments with Future e^+e^- Linear Colliders*, E. Fernandez and A. Pacheco (editors), UAB, Barcelona 2000, vol. I, 163 and hep-ph/9910271.
15. J. Brau, these proceedings.
16. V. Barger *et al.*, *Phys. Rev.* **D49** (1994) 79;
    K. Hagiwara and M.L. Stong, *Z. Phys.* **C62** (1994) 99.
17. A. Djouadi, J. Kalinowski and P.M. Zerwas, *Mod. Phys. Lett.* **A7** (1992) 1765 and *Z. Phys.* **C54** (1992) 255.
18. S. Dittmar *et al.*, *Phys. Lett.* **B441** (1998), 383 and *Phys. Lett.* **B478** (2000), 247;
    S. Dawson and L. Reina, *Phys. Rev. Lett.* **D57** (1998), 5851 and *Phys. Rev.* **D59** (1999), 054012 and S. Dawson, these proceedings.
19. A. Juste and G. Merino, in Proc. of the *Worldwide Study on Physics and Experiments with Future e^+e^- Linear Colliders*, E. Fernandez and A. Pacheco (editors), UAB, Barcelona 2000, vol. I, 265 and hep-ph/9910301.
20. J. Alcarez and E. Ruiz Morales, these proceedings and hep-ph/0012109
21. K. Desch and N. Meyer, these proceedings.
22. G. Borisov and F. Richard, Note LAL 99-26 and hep-ph/9905413.
23. M. Krawczyk, these proceedings.
24. G. Jikia and S. Söldner-Rembold, *Nucl. Phys. Proc. Suppl.* **82** (2000) 373,
25. E. Boos *et al.*, LC-PHSM-2000-053 and H.J. Schreiber *et al.*, these proceedings.
26. K. Desch and M. Battaglia, these proceedings.
27. A. Djouadi, M. Spira and P. Zerwas, *Z. Phys.* **70** (1996) 427;
    A. Djouadi, J. Kalinowski and M. Spira, *Comput. Phys. Commun.* **108** (1998), 56.
28. A. Djouadi *et al.*, *Eur. Phys. J.* **C10** (1999) 27 and
    M. Müehlleitner, these proceedings.
29. P. Gay, these proceedings.
30. G. Gounaris, A. Djouadi, H.E. Haber and P.M. Zerwas, *Phys. Lett.* **B375** (1996) 203; A. Djouadi *et al.*, *Eur. Phys. J.* **C10** (1999) 27 and M. Mühlleitner, these proceedings.
31. S. Heinemeyer, W. Hollik and G. Weiglein, *Phys. Lett.* **B440** (1998), 296 and *Phys. Rev.* **D58** (1998) 091701;
    S. Heinemeyer, W. Hollik and G. Weiglein, *Comput. Phys. Commun.* **124** (2000) 76.
32. A. Kiiskinen, M. Battaglia and P. Pöyhönen, these proceedings.
33. A. Andreazza and C. Troncon, DESY-123-E, 417.
34. M. Müehlleitner, these proceedings.
35. E. Asakawa, these proceedings.
36. D. Zeppenfeld *et al.*, *Phys. Rev.* **D62** (2000) 13009.
37. C. Ankenbrandt *et al.*, *Phys. Rev. ST Accel. Beams* **2** (1999) 081001 (1999)
38. *Prospective Study of Muon Storage Rings at CERN*, B. Autin, A. Blondel and J. Ellis (editors), CERN-99-02.